Adv. Radio Sci., 10, 183–186, 2012
www.adv-radio-sci.net/10/183/2012/
doi:10.5194/ars-10-183-2012

Advances in
Radio Science

An improved electrical and thermal model of a microbolometer for electronic circuit simulation

D. Würfel and H. Vogt

Fraunhofer Institute for Microelectronic Circuits and Systems, Duisburg, Germany

Correspondence to: D. Würfel (daniel.wuerfel@ims.fraunhofer.de)

Abstract. The need for uncooled infrared focal plane arrays (IRFPA) for imaging systems has increased since the beginning of the nineties. Examples for the application of IRFPAs are thermography, pedestrian detection for automotives, fire fighting, and infrared spectroscopy. It is very important to have a correct electro-optical model for the simulation of the microbolometer during the development of the readout integrated circuit (ROIC) used for IRFPAs. The microbolometer as the sensing element absorbs infrared radiation which leads to a change of its temperature due to a very good thermal insulation. In conjunction with a high temperature coefficient of resistance (TCR) of the sensing material (typical vanadium oxide or amorphous silicon) this temperature change results in a change of the electrical resistance. During readout, electrical power is dissipated in the microbolometer, which increases the temperature continuously. The standard model for the electro-optical simulation of a microbolometer includes the radiation emitted by an observed blackbody, radiation emitted by the substrate, radiation emitted by the microbolometer itself to the surrounding, a heat loss through the legs which connect the microbolometer electrically and mechanically to the substrate, and the electrical power dissipation during readout of the microbolometer (Wood, 1997). The improved model presented in this paper takes a closer look on additional radiation effects in a real IR camera system, for example the radiation emitted by the casing and the lens. The proposed model will consider that some parts of the radiation that is reflected from the casing and the substrate is also absorbed by the microbolometer. Finally, the proposed model will include that some fraction of the radiation is transmitted through the microbolometer at first and then absorbed after the reflection at the surface of the substrate. Compared to the standard model temperature and resistance of the microbolometer can be modelled more realistically when these higher order effects are taken into account. A Verilog-A model for electronic circuit simulations is developed based on the improved thermal model of the microbolometer. Finally, a simulation result of a simple circuit is presented.

1 Introduction

Far infrared (FIR) imager detect the IR-radiation of a warm body in the wavelength range between 8 and 14 µm passively, i.e. no further illumination is necessary. Usually in low cost systems an array of uncooled microbolometers as the sensor elements are used. Typical applications of IRFPAs are thermal imaging and pedestrian detection for automotive driving assistance systems, fire fighting, biological imaging, or military applications like target recognition (Würfel et al., 2011).

2 The microbolometer

The microbolometer is a temperature dependent resistor. It consists of a membrane which is suspended by two small legs from the CMOS substrate. The legs also contact the membrane electrically. The microbolometer absorbs the incoming infrared radiation and converts it into heat energy, which induces a temperature rise. This results in a change of the electrical resistance. Figure 1 shows a SEM image of a microbolometer fabricated by postprocessing on CMOS wafers at the Fraunhofer Institute for Microelectronic Circuits and Systems (Fraunhofer IMS) "Microsystem Lab & Fab" (Weiler et al., 2011). The sensor material used for the membrane is amorphous silicon. A vacuum package is required to reduce thermal losses by gas convection.

Published by Copernicus Publications on behalf of the URSI Landesausschuss in der Bundesrepublik Deutschland e.V.

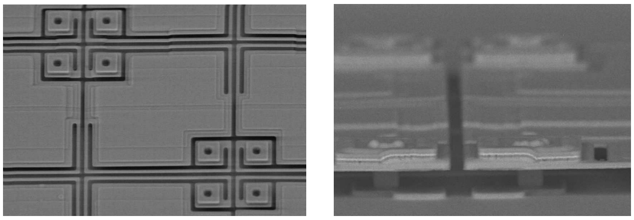

Fig. 1. SEM image of a microbolometer fabricated at the Fraunhofer IMS (left: top view, right: side view) (Weiler et al., 2011).

3 The Heat Balance Equation

A single microbolometer detects radiation power according to Fig. 2. The amount of incoming radiation power P_{Str} depends on the solid angle θ (Wood, 1997):

$$P_{\mathrm{Str}} = \pi L_{\mathrm{Str}} A_{\mathrm{Bolo}} \sin^2\theta, \tag{1}$$

where L_{Str} is the radiance and A_{Bolo} is the absorbing microbolometer area. With the definition of the F-number F_{no} (Wood, 1997)

$$F_{\mathrm{no}} = \frac{1}{2\sin\theta} \tag{2}$$

the power which is absorbed by a single microbolometer is given by

$$Q_{\mathrm{Str}} = \frac{\pi L_{\mathrm{Str}} A_{\mathrm{Bolo}} \varepsilon_{\mathrm{Bolo}}}{4F_{\mathrm{no}}^2}, \tag{3}$$

where $\varepsilon_{\mathrm{Bolo}}$ is the emissivity of the microbolometer. The microbolometer heats up during readout due to the electrical power dissipation by applying a voltage U_{Bias} and a very good thermal insulation. The incoming radiation power P_{Str} from a blackbody and the substrate are absorbed. Through the small legs, which connect the microbolometer to the substrate, heat energy with the substrate is exchanged. The microbolometer itself is also a radiation source. In direction of the lens and additional to the substrate radiation is emitted according to Stefan Boltzmann's law. A heat balance equation which describes the microbolometer temperature T when energy is exchanged is derived by (Wood, 1997):

$$c_{\mathrm{Bolo}} \frac{\mathrm{d}T}{\mathrm{d}t} = U_{\mathrm{Bias}} I_{\mathrm{Bolo}} + \varepsilon_{\mathrm{Bolo}} P_{\mathrm{Str}} + \varepsilon_{\mathrm{Bolo}} P_{\mathrm{sub}} - g_{\mathrm{Bolo}}(T_{-}T_{\mathrm{sub}}) - 2A_{\mathrm{Bolo}}\varepsilon_{\mathrm{Bolo}}\sigma T^4 \tag{4}$$

where c_{Bolo} is the microbolometer's heat capacitance, I_{Bolo} is the current through the microbolometer resistance, $\varepsilon_{\mathrm{Bolo}} P_{\mathrm{sub}}$ is the absorbed radiation power from the substrate, g_{Bolo} is the thermal conductance, T_{sub} is the substrate temperature and σ is the Stefan Boltzmann's constant.

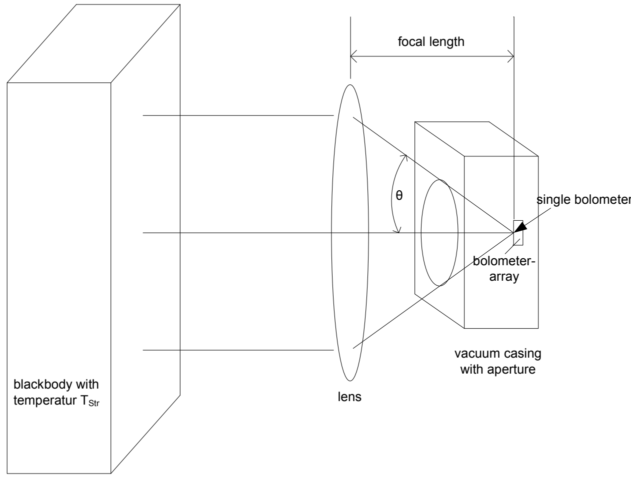

Fig. 2. Optical path from blackbody to the microbolometer, based on (Wood, 1997).

4 The enhanced heat balance equation

When using the heat balance Eq. (4) it showed out that there is an energy loss. For example, the microbolometer temperature T decreases, when microbolometer temperature T, blackbody temperature T_{Str}, and substrate temperature T_{sub} are equal at time $t = 0$ s without any electrical power dissipation. According to Eq. (4) for an emissivity $\varepsilon_{\mathrm{Bolo}} \approx 0.9$ of a microbolometer and a substrate emissivity $\varepsilon_{\mathrm{Bolo}} \approx 0.2$ with $T_{\mathrm{sub}} = T_{\mathrm{Str}} = T$ at time $t = 0$ s the microbolometer emits more power to the substrate P_{out} than it gets back. It emits in direction of the substrate

$$P_{\mathrm{out}} = A_{\mathrm{Bolo}} \varepsilon_{\mathrm{Bolo}} \sigma T^4. \tag{5}$$

But it only gets back from the substrate

$$P_{\mathrm{in}} = \varepsilon_{\mathrm{Bolo}} A_{\mathrm{Bolo}} \varepsilon_{\mathrm{sub}} \sigma T_{\mathrm{sub}}^4 = \varepsilon_{\mathrm{Bolo}} A_{\mathrm{Bolo}} \varepsilon_{\mathrm{sub}} \sigma T^4, \tag{6}$$

which is smaller by factor of $\varepsilon_{\mathrm{sub}}$ compared to Eq. (5). The result is that the temperature T of the microbolometer decreases. The part of the radiation power which is not absorbed by the substrate cannot be lost. In reality a great amount of the radiation power emitted by the microbolometer to the substrate is reflected back to it. Then it is absorbed and the microbolometer gets back some of the radiation power emitted by itself. So the heat balance equation will be enhanced to make it more realistic by taking reflections and their absorptions into account. Additional the casing and the lens emits and reflects radiation. Between 8 µm and 14 µm the transmissivity of the lens is assumed to be 1. The lens is assumed to be an ideal blackbody for radiation between 0 and 8 µm wavelength and also from 14 µm to infinity. The microbolometer is assumed to have a transmissivity of 1-$\varepsilon_{\mathrm{Bolo}}$ and to be part of an array with an infinite expansion. The substrate temperature T_{sub}, the temperature

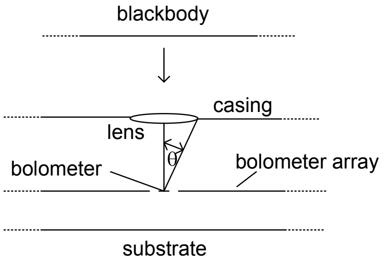

Fig. 3. Optical path from blackbody to the microbolometer.

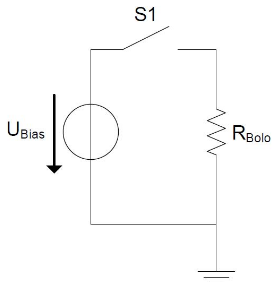

Fig. 4. Simple circuit used for simulation.

of casing and lens T_{cas} and T_{lens} respectively are constant. Thermal equilibrium is assumed.

An enhanced heat equation can now be derived (Würfel, 2010). The approach will be explained for the absorbed radiation power coming from the blackbody (Fig. 3). At first incoming radiation is absorbed as given by Eq. (7) according to Eq. (3), where P_{Str} is the radiation power for $\theta = \pi$, and P_{ab} is the radiation power coming through the lens to the surface of a microbolometer.

$$\begin{aligned} Q_{\mathrm{Str},1}(T_{\mathrm{Str}}) &= \varepsilon_{\mathrm{Bolo}} \frac{P_{\mathrm{Str}}(T_{\mathrm{Str}})}{4F_{\mathrm{no}}^2} \\ &= \varepsilon_{\mathrm{Bolo}} \frac{\pi A_{\mathrm{Bolo}} L_{\mathrm{Str}} T_{\mathrm{Str}}}{4F_{\mathrm{no}}^2} \\ &= \varepsilon_{\mathrm{Bolo}} P_{\mathrm{ab}}(T_{\mathrm{Str}}) \end{aligned} \tag{7}$$

The amount of radiation which was not absorbed by the microbolometer transmits to the substrate. Part of the radiation power is absorbed and the rest is reflected back in the direction to the microbolometer. Now there's another absorption in the microbolometer according to Eq. (8).

$$Q_{\mathrm{Str},2}(T_{\mathrm{Str}}) = \varepsilon_{\mathrm{Bolo}} P_{\mathrm{ab}}(T_{\mathrm{Str}})(1-\varepsilon_{\mathrm{Bolo}})(1-\varepsilon_{\mathrm{sub}}) \tag{8}$$

The part which is again not absorbed is transmitted in the direction of the lens and the casing. The part which now hits the lens is lost (compare with assumptions). The radiation power which hits the casing is absorbed partly. The rest is reflected in direction to the microbolometer. The F-number F_{no} of the lens is taken into account. In the microbolometer there is a third absorption according to Eq. (9).

$$\begin{aligned} Q_{\mathrm{Str},3}(T_{\mathrm{Str}}) &= \varepsilon_{\mathrm{Bolo}} P_{\mathrm{ein}}(T_{\mathrm{Str}})(1-\varepsilon_{\mathrm{cas}})(1-\varepsilon_{\mathrm{Bolo}})^2 \\ &\quad \cdot (1-\varepsilon_{\mathrm{sub}})\left(1-\frac{1}{4F_{\mathrm{no}}^2}\right), \end{aligned} \tag{9}$$

where $\varepsilon_{\mathrm{cas}}$ is the emissivity of the casing. In principle this is repeated infinitely. Of course the amount of radiation power gets smaller and smaller with each absorption. The final result is the sum of all absorption parts and given by Eq. (10).

$$\begin{aligned} Q_{\mathrm{Str}}(T_{\mathrm{Str}}) &= Q_{\mathrm{Str},1}(T_{\mathrm{Str}}) + Q_{\mathrm{Str},2}(T_{\mathrm{Str}}) + Q_{\mathrm{Str},3}(T_{\mathrm{Str}}) + \dots \\ &= \varepsilon_{\mathrm{Bolo}} \frac{\pi A_{\mathrm{Bolo}} L_{\mathrm{Str}}(T_{\mathrm{Str}})}{4F_{\mathrm{no}}^2} \cdot \left(1 + \sum_{n=1}^{\infty}\left[(1-\varepsilon_{cas})^n (1-\varepsilon_{\mathrm{Bolo}})^{2n}(1-\varepsilon_{\mathrm{sub}})^n \left(1-\frac{1}{4F_{\mathrm{no}}^2}\right)^n \right.\right. \\ &\quad \left.\left. + (1-\varepsilon_{\mathrm{cas}})^{n-1}(1-\varepsilon_{\mathrm{Bolo}})^{2n-1}(1-\varepsilon_{\mathrm{sub}})^n \left(1-\frac{1}{4F_{\mathrm{no}}^2}\right)^{n-1}\right]\right) \\ &= \varepsilon_{\mathrm{Bolo}} \frac{\pi A_{\mathrm{Bolo}} L_{\mathrm{str}}(T_{\mathrm{str}})}{4F_{\mathrm{no}}^2} \cdot \left(\begin{array}{l} \frac{1}{1-(1-\varepsilon_{\mathrm{cas}})(1-\varepsilon_{\mathrm{Bolo}})^2(1-\varepsilon_{\mathrm{sub}})\left(1-\frac{1}{4F_{\mathrm{no}}^2}\right)} + \\ + \frac{(1-\varepsilon_{\mathrm{cas}})^{-1}(1-\varepsilon_{\mathrm{Bolo}})^{-1}}{1-(1-\varepsilon_{\mathrm{cas}})(1-\varepsilon_{\mathrm{Bolo}})^2(1-\varepsilon_{\mathrm{sub}})\left(1-\frac{1}{4F_{\mathrm{no}}^2}\right)} + \\ -(1-\varepsilon_{\mathrm{cas}})^{-1}(1-\varepsilon_{\mathrm{Bolo}})^{-1} \end{array} \right) \end{aligned} \tag{10}$$

For all radiation sources the derivation can be done in a similar way. The enhanced heat balance equation is given by

$$\begin{aligned} c_{\mathrm{Bolo}} \frac{\mathrm{d}T(t)}{\mathrm{d}t} &= Q_{\mathrm{cas/lens}} + Q_{\mathrm{Str}}(T_{\mathrm{Str}}(t)) + Q_{\mathrm{sub}} - Q_{\mathrm{bolo}}(T(t)) \\ &\quad + Q_{\mathrm{array}}(T(t)) - Q_{\mathrm{leg}}(T(t)) + P_{\mathrm{elec}}(T(t)) \end{aligned} \tag{11}$$

where $Q_{\mathrm{cas/lens}}$ is the absorbed radiation power from the casing and lens, Q_{sub} is the absorbed radiation power from the substrate, Q_{bolo} is the emitted radiation power from the microbolometer (of course the reflected radiation at the substrate and casing/lens and the reabsorbed part is taken into account), Q_{array} is the absorbed radiation power from the other microbolometers in the array, Q_{leg} is the radiation power which is conducted to the substrate by the microbolometer's legs, and P_{elec} is the dissipated electrical power during readout. Using this equation a Verilog-A model for electronic circuit simulation has been developed. It acts as a temperature dependent resistor. The temperature is calculated numerically in dependence of the radiation power of the blackbody and the electrical power. Then the resistance changes according to the calculated temperature.

5 Simulation

The time dependent change of the bolometer temperature T for a bolometer used in a simple circuit (Fig. 4) is shown in Fig. 5. For this simulation a Verilog-A model for the resistor R_{Bolo} based on the described enhanced model of the heat balance equation has been used. The blackbody temperature T_{Str} is constant during this simulation. At time $t = 0$ s the readout switch $S1$ is closed and a readout current flows through the microbolometer resulting in an electrical readout power. After closing of the readout switch the microbolometer temperature increases. After some time the temperature reaches a constant value which dependents on the bias voltage U_{Bias}.

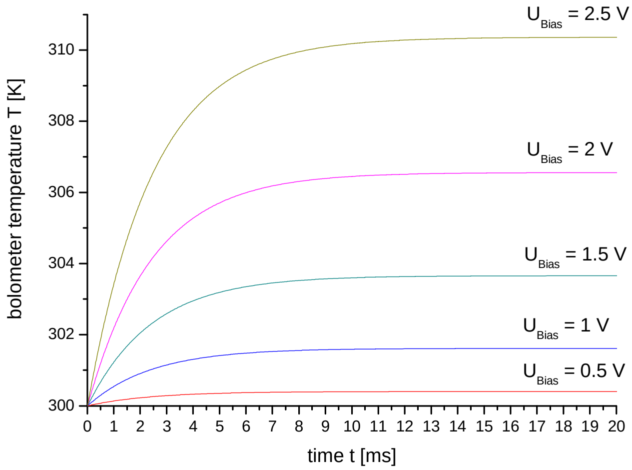

Fig. 5. Trend of microbolometer temperature with the parameter U_{Bias}.

6 Conclusions

The heat balance equation for a microbolometer as a sensor element for far infrared radiation derived by (Wood, 1997) has been enhanced to consider more effects in an IR camera system. The casing, lens, and the surrounding microbolometers are added as further radiation sources. Multiple reflections in an IR camera system have been taken into account. Also, some of the radiation that is reflected from the casing and the substrate is absorbed by the microbolometer. A Verilog-A model for a microbolometer resistance based on the enhanced heat balance equation has been developed. Finally, the result of a simulation of the bolometer temperature for a bolometer in a simple circuit using this Verilog-A model has been shown.

References

Weiler, D., Ruß, M., Würfel, D., Lerch, R., Yang, P., Bauer, J., Kropelnicki, P., Heß, J., and Vogt, H.: Improvements of a Digital 25μm Pixel-Pitch Uncooled Amorphous Silicon TEC-less VGA IRFPA with Massively Parallel Sigma-Delta-ADC Readout; Proc. of SPIE, Vol. 8012, 80121F-1-7, 2011.

Wood, R. A.: Monolithic Silicon Microbolometer Arrays; Uncooled Infrared Imaging Arrays and Systems, edited by: Kruse, P. and Skatrud, D., Semiconductors and Semimetals, 47, 45–121, Academic Press, 1997.

Würfel, D.,Ruß, M., Lerch, R., Weiler, D., Yang, P., and Vogt, H.: An Uncooled VGA-IRFPA with Novel Readout Architecture; Adv. Radio Sci., 9, 107-110, 2011, http://www.adv-radio-sci.net/9/107/2011/.

Würfel, D.: Rauscharme Ausleseschaltungen für die Infrarot-Sensorik; Dissertation, Universität Duisburg-Essen, 2010.